COMPARATIVE STUDIES OF INFRARED LASER AND RADIO-FREQUENCY ACTION ON IN VITRO BIOTISSUES BY THE METHOD OF POLARIZATION SENSITIVE OPTICAL COHERENCE TOMOGRAPHY

G. Yu. Golubyatnikov,[1] * M. A. Shakhova,[2]
L. B. Snopova,[2] A. B. Terent'yeva,[2]
N. Yu. Ignat'yeva,[3] and V. A. Kamensky[1]

UDC 535.55+615.844+681.784

We make comparative studies of structural changes of in vitro biotissues subject to the infrared (IR) laser radiation and the radio-frequency field. Noninvasive diagnostics and monitoring of microstructural changes of biological tissues are performed using optical coherent tomography.

1. INTRODUCTION

Fundamental problems of studies of the laser, radio-frequency, and microwave action on biotissues have become practical. Laser radiation is used for tissue resection with simultaneous coagulation of vessels, lithotripsy, and controlled removal of micron layers. The infrared laser and radio-frequency action is used for treatment of early-stage malignant tumors, which allows one to significantly improve the surgery efficiency and decrease postoperative complications. Laser heating is used for modifying the form and sizes of the collagen-containing tissues with simultaneous reaching of therapeutic or cosmetic effects (thermoplastics) and subsequent running of regeneration processes [1].

Use of high-frequency, or radio-frequency (RF) radiation for dissection and coagulation of tissues started in the 1920s in the pioneering works of W. T. Bovie, Harward University. Use of radar microwave oscillators in civil fields in the 1950s gave an impetus to the development of studies of the microwave influence on living organisms and biological systems [2, 3]. At present, diagnostics and therapy of cancerous tumors cannot operate without RF and microwave radiation [4].

Radio-frequency emission heats tissue to a larger depth compared with IR radiation. Moreover, the possibility of using arbitrarily shaped electrodes is a significant advantage of the RF heating. In this case, an increase in the density of absorbed energy is reached due to a decrease in the electrode size, and a sharp boundary between the electrode and tissue allows us to perform surgery with high accuracy, without serious damage of surrounding tissues. This determines wide use of this method in clinical medicine [5, 6].

The degree of the electromagnetic-radiation influence on tissue depends on its heating degree, which is determined by radiation absorption by water contained in almost all biotissue types. The following temperature regimes can be singled out: tissue heating up to 40–45 °C; coagulation and hyperthermia which occur as a result of heating up to 60–80 °C, along with the thermoplastics of connecting tissues occurring when the influence is usually due to contraction of the collagen fiber; ablation occurring at temperatures exceeding 100 °C, pyrolysis for which heating above 150 °C is required, and, as a result, dissection and perforation of tissues [7].

* glb@appl.sci-nnov.ru

[1] Institute of Applied Physics of the Russian Academy of Sciences; [2] Nizhny Novgorod State Medical Academy, Nizhny Novgorod; [3] M. V. Lomonosov Moscow State University, Moscow, Russia. Translated from Izvestiya Vysshikh Uchebnykh Zavedenii, Radiofizika, Vol. 53, No. 1, pp. 41–50, January 2010. Original article submitted July 3, 2009; accepted January 29, 2010.

Comparative studies of the developed laser and RF engineering methods, which would allow one to reasonably choose the required option of action and optimize the regime for cutting or modifying tissues with minimum postoperative complications, such as restenosis development because of the scar-tissue growth and granulations [8, 9], are insufficiently studied in the literature. Among the well-known comparative studies of various types of influences, we can mention work [10] dealing with myocardium perforation using the radiation from a CO_2-laser or an RF discharge.

This study is aimed at a comparative analysis of biotissue changes as a response to laser radiation with a wavelength of 1.56 μm and an RF electromagnetic field with a frequency of 3.8 MHz under monitoring of an option of polarization-sensitive optical coherence tomography (OCT), namely, cross-polarization OCT. This method allows one to obtain information not only on the object structure from the backscattered-signal characteristics, but also its damage when heated up to 50–110 °C by using variations in the tissue ability of birefringence and depolarization [11–13].

The tissue heating temperature in the experiments did not usually exceed 100 °C. This temperature regime is the most suitable for clarifying the mechanisms of the IR and RF action on the surrounding tissues since it is difficult to single out the differences between these kinds of action because of a pronounced damage such as carbonization in the resection regime when the heating temperature exceeds 300 °C.

The problem of optimizing operation regimes of a "Surgitron" RF device was solved on the basis of comparing changes in the tissues after the laser and RF heating, which were recorded by the OCT method.

2. MATERIALS AND METHODS

All experiments were conducted *ex vivo* with animal tissues such as tendons, intervertebral disks, ear cartilage, and nasal septal cartilage.

Laser processing of the tissue specimens was performed by emission of an LS-1.56 erbium fiber laser with a wavelength of 1.56 μm, manufactured by the "IRE-Polus" company (Russia). Laser radiation was supplied to the specimen surface via an optical fiber of 400 μm in diameter with a sapphire window at the end (the window diameter was 1 mm). The experiments were conducted in the pulsed-periodic irradiation regime with the output power varied from 0.1 to 6 W. Although the changeable optical attachments allowed one to vary the irradiated-zone size, it usually did not exceed 2 mm in the described experiments. The typical irradiation time was 3–10 s.

The RF heating of the tissues was performed by a "Surgitron FFPF EMC" radiosurgery device with a monopolar electrode whose description is available in the Internet [14]. Its output frequency and voltage were 3.8 MHz and up to 400 V, respectively. We also used additional disk electrodes with diameters from 1.5 to 6 mm, which allowed us to vary the electric-field intensity in the area of contact between the electrode and tissue. The voltage and current, as well as the matching degree between an RF oscillator and the load, i.e., biotissue specimens in our case, were measured by a Rogowski coil and a 5 Ω measuring resistor. Since the electric-field intensity depends on the distance between the electrode and the tissue surface, which can be nonuniform, and the electrode pressing degree, it is required to control the gap between the electrode and the sample surface. A 40-μm Teflon film was used for this purpose. This allowed us to significantly increase the heating stability and avoid sparks and the tissue-surface burning.

The sample temperature of the specimen surface was measured by a Chromel–Alumel thermocouple of 1 mm in diameter and an IR pyrometer manufactured by the "Optris, LaserSight" company (Germany) with a minimum spatial resolution of 1 mm at a distance of 62 mm and operation spectral range 8 to 14 μm. The variation dynamics of the tissue subsurface temperature was recorded by a PC. Comparing the temperatures obtained by these methods, we see that the temperature can adequately be measured by an IR pyrometer if the tissue-emission coefficient is about 0.95.

To monitor the biotissue microstructure changes, we used the cross-polarization OCT device manufactured at the Institute of Applied Physics of the Russian Academy of Sciences (Nizhny Novgorod, Russia) [15], whose diagram is shown in [16]. It allows us to obtain the optical image of the object simultaneously in direct and orthogonal polarization [17, 18]. The radiation wavelength of the superluminescent diode used

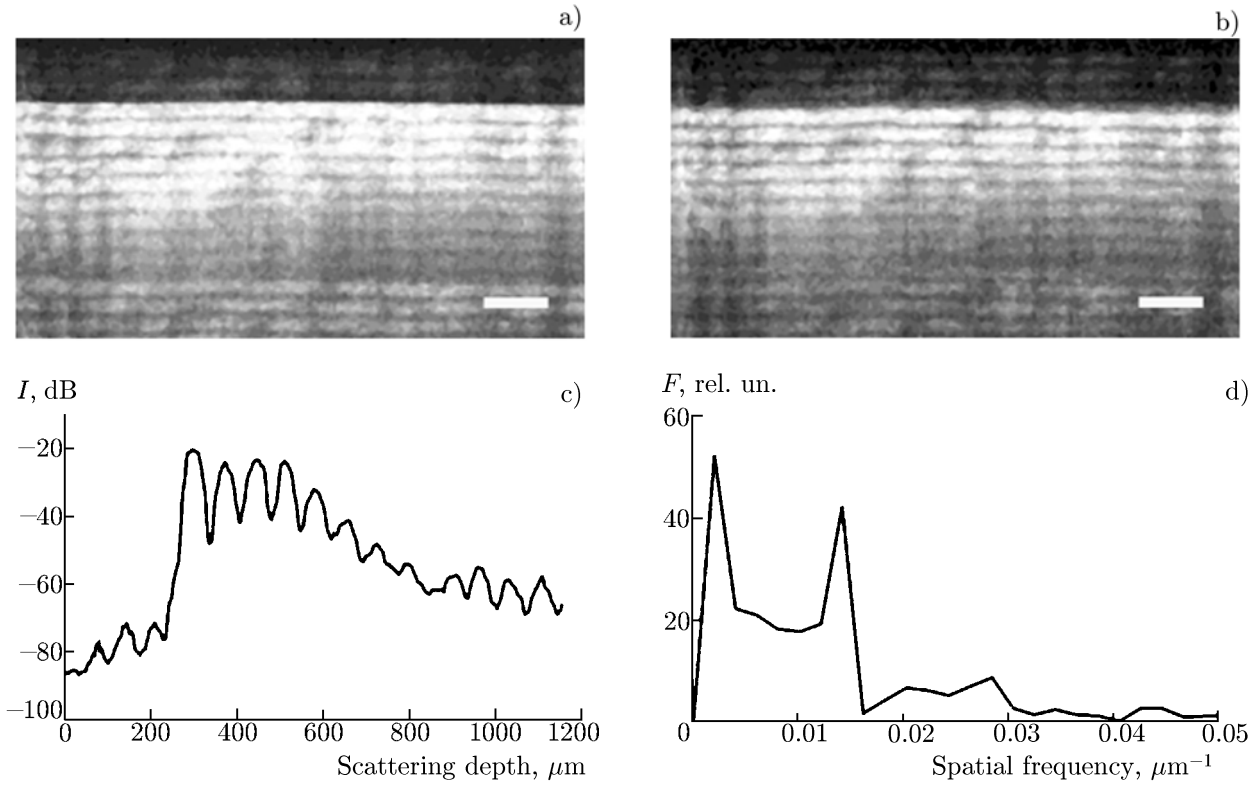

Fig. 1. OCT images of intact tissue of the cow vertebral bands for direct (*a*) and orthogonal (*b*) polarizations, the relative distribution of the intensity I of the scattered orthogonal-polarization signal as a function of depth (*c*), and its Fourier transform F (*d*). The spectral peaks correspond to the spatial periods 400 and 70 μm, and the white band corresponds to 250 μm.

as a source was 980 nm and the spectral width of emission was 60 nm. These parameters determined the spatial resolution with respect to depth, which was 15 μm. This diagnostics can be assumed noninvasive since the power of radiation acting on the object does not exceed 1 mW. The tomograph is equipped with a flexible optical fiber probe with an optical-scanner end window of 2.7 mm in diameter and a transverse resolution of 25 μm. When scanning the area of interest, the probe was brought in contact with the studied object. The scanned area contains 200 dots in the transverse direction and 300 dots for the depth, which corresponds to a 2.2×1.6 mm area for air whose refractive index $n = 1$. The lightest black-and-white OCT-image portions correspond to the maximum signal intensity, while the darkest portions correspond to the minimum intensity (Figs. 1*a* and 1*b*).

For collagen-containing tissues, birefringence, whose characteristics in general case depend on the wavelength, is due to the ordered uniaxial packing of the rod-like molecules of this protein into fibrils and fibers. When an electromagnetic wave is scattered by such a structure, the polarization-vector angle is rotated. Anisotropic properties lead to the appearance of an interference pattern in the received signal, which is seen in the tomograms as a regular alternation of the dark and light bands. The difference Δn of the refractive indices for the orthogonal polarizations is the quantitative characteristic of anisotropy. The tissue heating initiates some processes including variation in the water concentration, decomposition of proteoglycans and their associates with collagen fibrils, and conformational and supramolecular changes in the collagen subsystem. This leads to a variation in the degree of anisotropy Δn, which manifests itself as widening or narrowing of the interference bands. Therefore, cross-polarization OCT is an extremely sensitive method for diagnostics of small modifications in tissues, which especially refers to connective tissues.

The measurement procedure involved several stages, namely, choosing the intact tissue part whose structure most precisely reflects the features of the chosen tissue with the help of recording of OCT images,

the action of the RF or laser-emission influence on the chosen area, and recording of the OCT image of this area.

As an example, Fig. 1 shows the images of intact tissue of the cow vertebral bands, which were obtained by the OCT method for the direct (*a*) and orthogonal (*b*) polarizations. Figure 1*c* shows the ratio of the intensities of the backscattered and incident signals in decibels as a function of the scattering depth. The presented distribution was obtained by averaging over 10 points symmetrically located with respect to the tomogram cross section corresponding to the transverse coordinate 1.43 mm in Fig. 1*b*. Figure 1*d* shows the corresponding Fourier transform. It should be noted that for clarity the Fourier transform is calculated without the constant component of the depth distribution of the reflected-signal amplitude. Therefore, the first spectral peak in Fig. 1*c* has no physical meaning, but can be used for estimating the rate of the scattered-signal decrease with depth, which is about 25 cm^{-1} and determined by the extinction coefficient, i.e., the sum of the absorption and scattering coefficients, and the geometry of the mutual location of the radiation source and receiver.

Period $\Delta z = 70$ μm of the interference bands of the scattered signal, which result from birefringence, corresponds to the difference $\Delta n = \lambda/(2\,\Delta z) = 7 \cdot 10^{-3}$ of the refractive indices for orthogonal polarizations. It can be determined directly from the spatial frequency that corresponding to the second peak, in the amplitude distribution or its Fourier transform.

The absorption and scattering coefficients for various tissues are fairly well studied (see, e.g., [19]). The absorption coefficient at this wavelength is primarily determined by the water and hemoglobin content in tissues or water content in cartilaginous tissues and is at least an order of magnitude lower than the scattering coefficient $\mu_\mathrm{s} > 10$ cm^{-1}. Therefore, recovery of the scattering coefficient from the reflected signal can give us an additional possibility of differentiation of the tissue structure [20, 21]. The refractive index of the tissue was determined by thin sections of cartilaginous tissues with known thickness not exceeding 1 mm. The mean refractive index for cartilaginous tissues in these experiments was $\langle n \rangle \approx 1.41 \pm 0.20$.

Morphological verification of the optical data was performed by a standard method, i.e., using the hematoxylin and eosin (HE)staining and Van Gieson's staining.

3. MAIN RESULTS

The studies of the structural changes in the cartilaginous tissues during the LS-1.56 laser heating up to 60–80 °C, which were conducted under monitoring by cross-polarization OCT, on the whole reproduced the results previously obtained in [22, 23], where the collagen denaturation degree was determined by the method of differential scanning calorimetry. In this paper, the regimes of the laser action on connective tissues for the partial collagen denaturation and the RF action regimes were optimized and comparative analysis of the two heating methods was performed.

Figure 2 shows typical OCT images of the portions of both intact tissue (Fig. 2*a*) and the tissue after the laser irradiation (Figs. 2*b*–2*d*). Analysis of the OCT images shows that changes in the tissues after the laser irradiation are confined to a depth of about 1 mm, which corresponds to the water-absorption coefficient 9.65 cm^{-1}. The tomograms in Figs. 2*b* and 2*c* show the dependence of the degree of the structural change on the pulse duration, which was 100 and 300 ms, respectively. The time between the pulses was 300 ms. The observed difference is most probably related to the temperature dependence of the heat conduction and diffusion of water in tissues.

The tomogram in Fig. 2*d* shows the collagen-fiber melting in the laser-irradiation zone. The reached maximum temperature averaged over the surface of this zone with a diameter of about 1.5 mm did not exceed 80 °C, which was sufficient for the collagen macromolecule transformation from the triple helix to a random glomus and destruction of the ordered organization of the fibrils and fibers, i.e., denaturation.

It was much more difficult to obtain quantitative data in the case of RF heating since to determine the electric-field value and its characteristic variation scale over the tissue depth, we should allow for the electrode geometry and size, as well as the tissue permittivity and conductivity. In addition, one should take into account such factors as the surface state, the potential drop due to the subsurface-layer resistance,

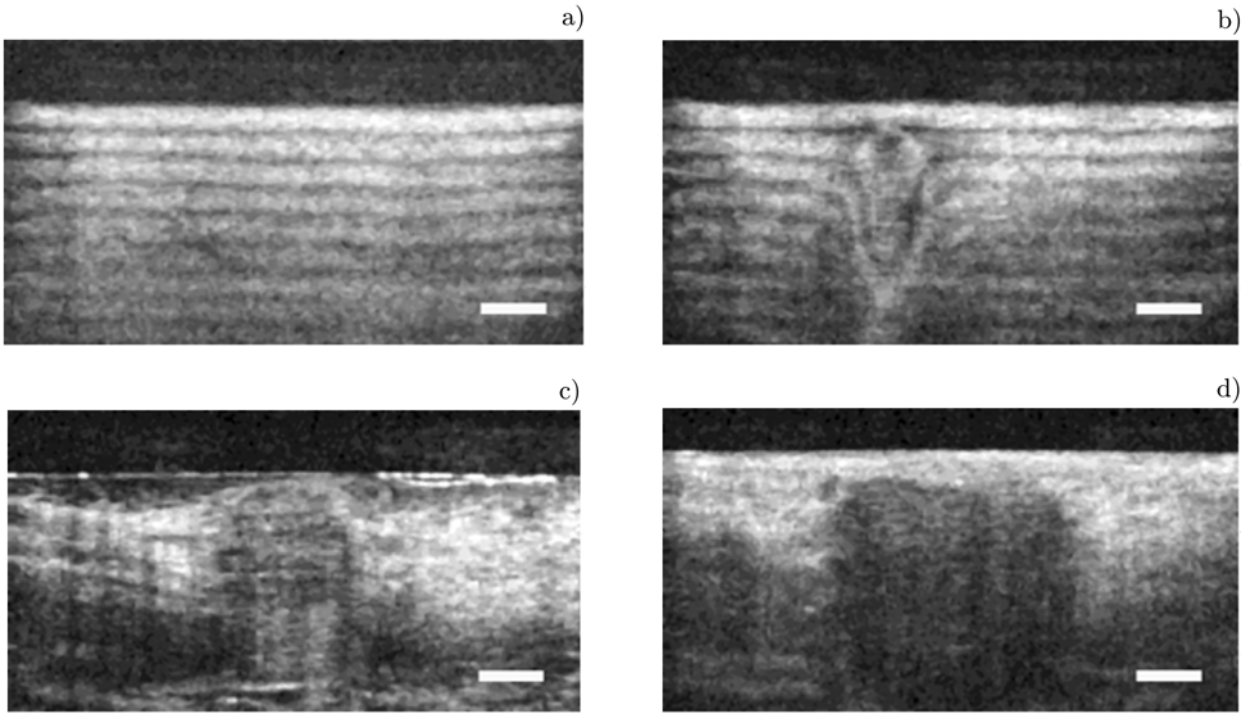

Fig. 2. OCT images of intact tissue before and after the laser irradiation for the wavelength 1.56 μm and the following laser irradiation regimes: orthogonal-polarization signal before (*a*) and after (*b*) irradiation for the maximum power $P_{\max} = 0.7$ W, pulses with 300-ms duration and 300-ms pause, and the irradiation duration $T = 5$ s; the direct-polarization signal after the laser irradiation (*c*) with $P_{\max} = 2.1$ W, pulses with 100-ms duration and 300-ms pause, and $T = 5$ s, and the same (*d*) for $P_{\max} = 2$ W with 300-ms pulses and 300-ms pauses and $T = 5$ s. The white band corresponds to 250 μm.

and the inhomogeneity of the tissue itself. Nevertheless, to predict the RF heating degree of a tissue in the given uniform field for a low power, i.e., in the linear regime, one can use the values of permittivity and the loss tangent for different types of human tissues, published in [24, 25] and also in [26].

In this paper, we tried to control the RF irradiation dose using the "Surgitron" device for the tissue modification. However, solving this problem by direct monitoring of the surface temperature in real time is extremely difficult since the standard thermocouple sensor can hardly be used for this purpose because of the presence of a strong spurious signal from an RF oscillator. The infrared pyrometer is resistant to the RF-field noise, but it yields the mean temperature in the range corresponding to the spatial resolution of the pyrometer. Note that the fiber-optic thermometric sensor is most suitable for measuring the local temperature in tissues in the presence of the RF or microwave radiation.

The RF field was created by the operating electrode with respect to the insulated reference electrode in the form of a rectangular 10×15 cm plate (the supply wire length was about 2 m) placed under the object. When the operating electrode was applied to the biological object, a small variation in the electrode impedance of the order of 10 % was observed, which was mainly related to the introduced capacitance of the biological object. For the output voltage 400 V, the measured current did not exceed 0.4–0.5 A, i.e., the absolute value of the impedance at a frequency of 3.8 MHz was about 1000 Ohm, which corresponded to the value 50–100 pF of the measured electrode capacitance in air. The power loss of the RF radiation during the biotissue heating occurs only near the operating-electrode surface. For example, for the tissue-heating power of the order of 2 W, which is a typical laser-heating power, variation in the active resistance of electrodes corresponds to 10 Ohm, or variation in the current phase with respect to the voltage phase by less than 1 deg. Therefore, it is rather difficult to monitor the dynamics of variations in the active loss, which is introduced by the biological object during the heating, by measuring the impedance in real time.

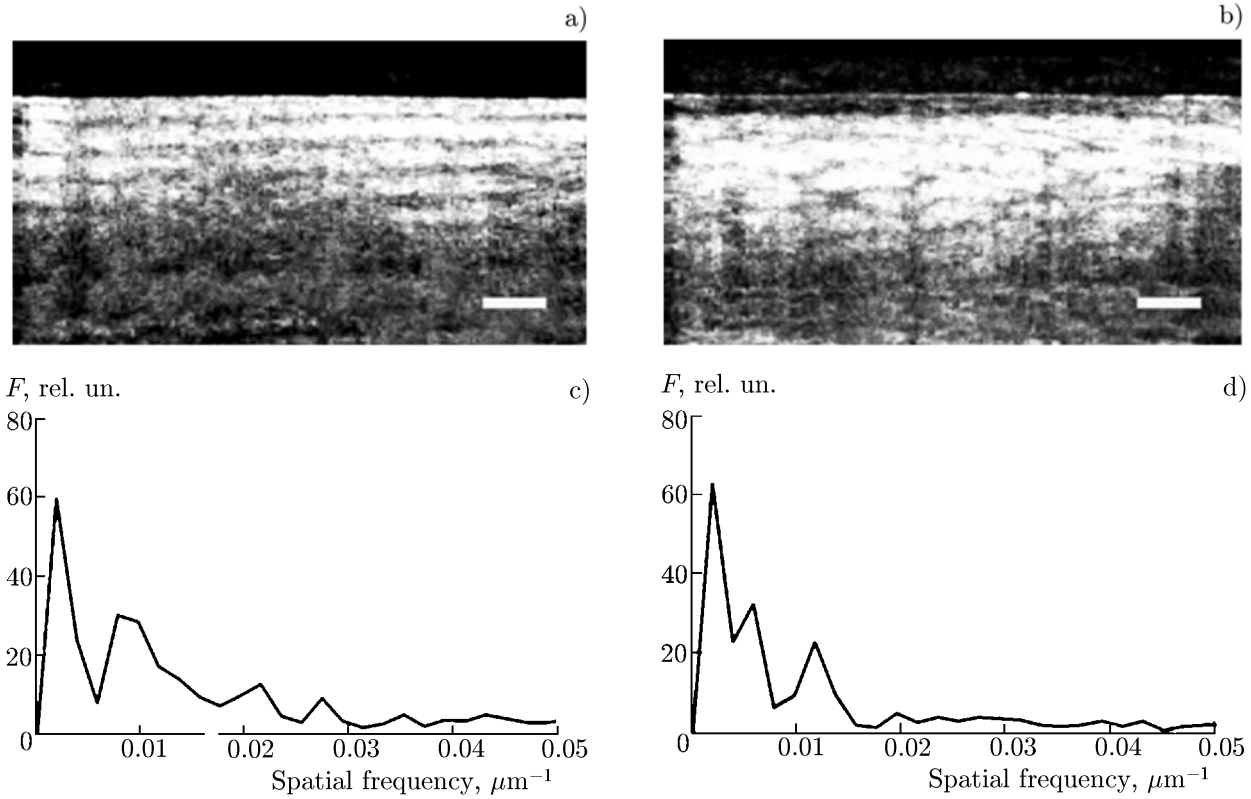

Fig. 3. OCT image of the hen shin tendon before (*a*) and after (*b*) RF irradiation. The corresponding Fourier transforms F of the scattered signal are shown in the lower part of the figure for the tomogram cross section which corresponds to the transverse coordinate equal to 1.4 mm; the characteristic spatial interference periods are equal to 110 μm for intact tissue and 172 83 μm after the RF irradiation. The white strip corresponds to 250 μm.

Therefore, the absorbed-energy dose of the RF radiation was estimated by comparing the changes in tissues, recorded by cross-polarization OCT, after the RF and laser irradiation. In this case, the OCT method was also used for determining the scale and character of the tissue-damage region. The heating dynamics was determined from the OCT tomograms for different action times. As a rule, a sharp change in the tissue-damage character with increasing RF action time was observed, which indicates the nonlinear character of heating. For the used laser powers 0.5–2.0 W, the irradiation dose corresponding to collagen denaturation usually did not exceed 5 J (see Fig. 2*d*). Choosing the RF action regime leading to similar changes in approximately the same tissue volume, we can estimate the RF irradiation dose, which also should not exceed 5 J in this case.

The OCT images shown in Fig. 3 demonstrate changes in the hen tendon tissue after the RF irradiation with a 10-s exposure. As was previously noted, an additional potential drop occurs in a subsurface layer with a thickness of about 100 μm, which leads to pronounced changes in the scattered signal on the tomogram in Fig. 3*b*. The corresponding birefringence spatial spectra are shown in the lower part of Fig. 3. The spatial modulation period of the interference signal amounts to 110 μm for intact tissue (Fig. 3*c*). After the RF irradiation, significant changes in the quantitative characteristics of this quantity occur. In particular, two peaks corresponding to the characteristic periods 83 and 172 μm (see Fig. 3*d*) are observed in the interference spectrum. In this case, a change in the interference period is related not only to changes in the birefringence properties of the tissue, but also to changes in the mean value of the refractive index, according to the morphological studies.

Stratification and disruption of collagen fibers over the entire irradiated area is revealed during the histological study of the tendon structure after the RF action (Fig. 4). Nonuniform basophilia of fibers with

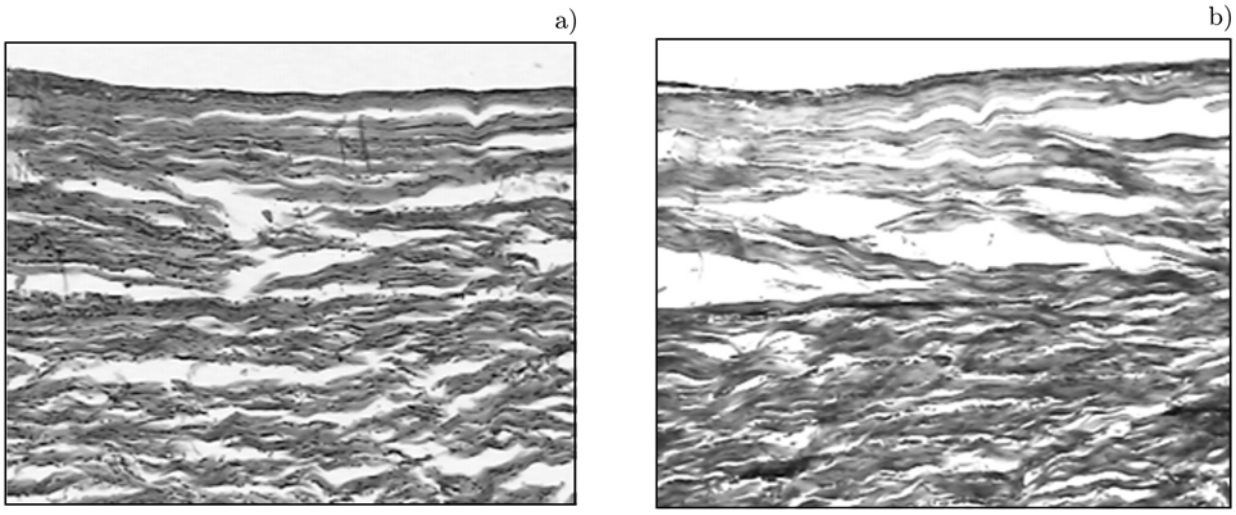

Fig. 4. Hen tendon structure after the RF irradiation, which corresponds to the OCT images of a tissue portion in Fig. 3 for HE stain (*a*) and Van Gieson's stain (*b*); the image scale is 1×1 mm.

normal-stain portions is observed in the case of HE stain. Correspondingly, in the case of Van Gieson's stain, one can observe nonuniform staining of fibers by fuchsin and portions which do not accept fuchsin. The above changes seem to reflect the selective denaturation of collagen in individual fiber bundles or their parts. Visually, on histological sections, unchanged fibers alternate with denaturated fibers, which can be confirmed by impaired acceptance of the applied stains.

Unlike the case of laser treatment where the tissue in the heating region is uniform, the presence of microdisruptions the distance between which in tissues after the RF action is 50 μm or longer by depth indicates a small-scale nonuniformity of the RF heating. The used frequency 3.8 MHz belongs to the range in which the loss is determined by the ion conductance of tissues. The loss value increases with increasing temperature [27]. The nonlinear regime of absorption of the intense RF field by water contained in tissues leads to the development of a thermal instability and determines the local overheating. The nonlinear behavior of irradiation was confirmed by the OCT tomograms: a "sharp" collagen melting was observed when the voltage or irradiation dose were increased, i.e., the birefringence effect disappeared in the narrow channel under the electrode. The tissue drying was observed for a small electric-field intensity with increasing heating time.

4. CONCLUSIONS

We demonstrated the effectiveness of comparative studies and the possibility of optimizing the regimes of both laser and RF action under the cross-polarization OCT monitoring. It is shown that cross-polarization OCT allows one to detect the features of the biotissue response depending on the action type.

The cross-polarization OCT monitoring of the laser and RF action showed the essentially different dynamics of the processes during the above irradiation. The RF heating determined by the tissue water is nonuniform and the heating-nonuniformity scale is of the order of 50 μm. For high powers, this leads to a change in the tissue resection character and the tissue disruption by the internal water pressure, which was observed in the OCT images and confirmed by histological studies. Therefore, the "Surgitron" device is primarily intended for the tissue cutting and ablation. To solve the problems of the tissue hyperthermia and thermoplastics, we should change the RF irradiation regimes, for example, use the pulsed-periodic oscillation regime with a shortened pulse duration.

We sincerely thank the research workers of Nizhny Novgorod State Medical Academy for support of the studies.

This work was supported by the Russian Foundation for Basic Research (project Nos. 06–08–00950-a, 10–02–00748-a, 10–02–01142-a, and 09–02–97097-r-povolzh'e-a)

REFERENCES

1. V. N. Bagratashvili, E. N. Sobol', and L. B. Shekhter, eds., *Laser Engineering of Cartilages* [in Russian], Fizmatlit, Moscow (2006).
2. A. S. Presman, *Sov. Phys. Uspekhi*, **6**, No. 3, 463 (1965).
3. J. H. Bernhardt, *Phys. Med. Biol.*, **37**, No. 4, 807 (1992).
4. A. Rosen, H. D. Rosen, and S. D. Edwards, in: M. Golio, ed., *The RF and Microwave Handbook*, CRC Press, Boca Raton, Fl. (2001).
5. I. F. Comaish and M. A. Lawless, *J. Cataract Refractive Surg.*, **29**, No. 1, 202 (2003).
6. R. Fitzpatrick, R. Geronemus, and G. Goldberg, *Lasers Surg. Med.*, **33**, 232 (2003).
7. H.-P. Berlien and G. J. Müller, eds., *Applied Laser Medicine*, Springer-Verlag, Berlin (2003).
8. A. V. Shakhov, A. B. Terentjeva, and V. A. Kamensky, *J. Surg. Oncol.*, **77**, 253 (2001).
9. R. M. Jovic, B. Baros, D. Duric, et al., *Med. Pregl.*, **59**, Nos. 7–8, 309 (2006).
10. V. S. Kazakevich, S. V. Kayukov, L. G. Mikheeva, et al., *Izv. Sib. Nauchn. Tsentr. Rossiisk. Akad. Nauk*, **5**, No. 1, 137 (2003).
11. J. F. de Boer, S. M. Srinivas and A. Malekafzabi, *Opt. Express*, **3**, 212 (1998).
12. M. C. Pierce, R. L. Sheridan, B. H. Park, et al., *Burns*, **30**, 511 (2004).
13. K. Schoenenberger, B. W. Colston, Jr., D. J. Maitland, et al., *Appl. Opt.*, **37**, 6026 (1998).
14. www.ellman.com/products/medical/radiosurgical_units.htm.
15. V. Kamensky, F. Feldchtein, V. Gelikonov, et al., *J. Biomed. Opt.*, **4**, No. 1, 137 (1999).
16. R. V. Kuranov, V. V. Sapozhnikova, N. M. Shakhova, et al., *Quantum Electron..*, **32**, No. 11, 993 (2002).
17. R. V. Kuranov, V. V. Sapozhnikova, I. V. Turchin, et al., *Opt. Express*, **10**, No. 15, 707 (2002).
18. V. M. Gelikonov and G. V. Gelikonov, *Laser Phys. Lett.*, **3**, 445 (2006).
19. http://omlc.ogi.edu/spectra/.
20. D. A. Zimnyakov and V. V. Turchin, *Quantum Electron..*, **32**, No. 10, 849 (2002).
21. I. V. Turchin, E. A. Sergeeva, L. S. Dolin, et al., *J. Biomed. Opt.*, **10**, No. 6, 064024 (2005).
22. N. Yu. Ignatieva, O. L. Zakharkina, I. V. Andreeva, et al., *Photochem. Photobiol.*, **83**, 675 (2007).
23. N. Yu. Ignatieva, O. L. Zakharkina, É. N. Sobol', et al., *Doklady Biochem. Biophys.*, **413**, Nos. 1–6, 92 (2007).
24. C. Gabriel, S. Gabriel, and E. Corthout, *Phys. Med. Biol.*, **41**, 2231 (1996).
25. S. Gabriel, R. W. Lau, and C. Gabriel, *Phys. Med. Biol.*, **41**, 2251 (1996).
26. http://niremf.ifac.cnr.it.
27. M. A. Esrick and D. A. McRae, *Phys. Med. Biol.*, **39**, 133 (1994).